Influence of liquefaction on scour behind coastal dikes due to tsunami overflow

Takegawa, Naoki
Sawada, Yutaka
Murai, Kazuki
Kawabata, Toshinori

(Citation)
International Journal of Geotechnical Engineering,12(1):40-45

(Issue Date)
2018-01-02

(Resource Type)
journal article

(Version)
Accepted Manuscript

Influence of Liquefaction on Scour behind Coastal Dikes due to Tsunami Overflow

Naoki TAKEGAWA: Student

Graduate School of Agricultural Science, Kobe University, Kobe, Japan

(1-1 Rokkodai, Nada, Kobe, Hyogo, 657-8501, Japan)

Email: 164a009a@stu.kobe-u.ac.jp

Yutaka SAWADA: Assistant Professor, Corresponding author

Graduate School of Agricultural Science, Kobe University, Kobe, Japan

(1-1 Rokkodai, Nada, Kobe, Hyogo, 657-8501, Japan)

E-mail: sawa@harbor.kobe-u.ac.jp

Kazuki MURAI:

Graduate School of Agricultural Science, Kobe University, Kobe, Japan

(1-1 Rokkodai, Nada, Kobe, Hyogo, 657-8501, Japan)

E-mail: kazuki_murai@water.go.jp

Toshinori KAWABATA: Professor

Graduate School of Agricultural Science, Kobe University, Kobe, Japan

(1-1 Rokkodai, Nada, Kobe, Hyogo, 657-8501, Japan)

E-mail: kawabata@kobe-u.ac.jp

Influence of Liquefaction on Scour behind Coastal Dikes due to Tsunami Overflow

In the present study, hydraulic model experiments were conducted to clarify the influence of liquefaction on the scour behind coastal dikes due to tsunami overflow. In particular, the variation of the scour profile (scour depth, scour length and scour area) due to liquefaction was discussed. Degree of liquefaction was controlled by upward seepage, which was induced by the head difference between a water tank and a sand bed. Six hydraulic gradients were applied to the sand bed. The experimental results showed that liquefaction had a significant impact on the scour profile. At high hydraulic gradient, slope failures occurred due to reduction of effective stress of the sand bed. As a result, scour length was increased by the slope failures. Furthermore, the maximum scour depth and scour area for high hydraulic gradient became smaller than that for low hydraulic gradient.

Keywords: coastal dike; tsunami overflow; scour; liquefaction; model experiment

Introduction

An earthquake occurred off the Pacific coast of Tohoku on 11th March 2011, which triggered massive tsunami waves of 10 m or more. The tsunami caused severe damage to coastal structures, such as coastal dikes and seawalls. After the earthquake, field surveys were conducted by Kato et al. (2012), Kawasaki (2012), Mikami et al. (2012), Tokida and Koizumi (2011) and Tokida and Tanimoto (2014). Scour holes caused by tsunami were found behind coastal dikes, as shown in Fig. 1. Scour behind coastal dikes caused the destabilization of coastal dikes and sliding of scour protections. Therefore, scour behind the coastal dikes has been considered as one of the reasons of their failures.

Fig.1.

Many studies on the scour behind coastal dikes have been conducted. Mitobe et al. (2014) conducted hydraulic model experiments to clarify the characteristics of the scour behind a coastal dike. Two flow fields at scour holes were observed and the scour

process was completely different depending on the flow field. Hatogai et al. (2008), Iiboshi et al. (2014) and Iiboshi et al. (2015) examined the scour process behind a coastal dike and the effects of scour protections. These studies revealed that scour protections changed the direction of the overflow water, and a scour hole developed away from the coastal dike. Tanimoto and Tokida (2012) reported that the scour hole that appeared behind coastal dikes caused dike failures but reduced the impact of the tsunami. The analytical tsunami simulations were conducted to verify the reduction of the tsunami by the scour hole. It was indicated that the tsunami's flow velocity was reduced by approximately 40%. In the 2011 earthquake off the Pacific coast of Tohoku, liquefaction occurred widely in the Kanto region. Conversely, there were not many reports of liquefaction in the Tohoku coastal areas. One reason is that the tsunami obliterated the traces of liquefaction. However, many researchers pointed out that liquefaction did in fact occur in these coastal areas. Fukumoto et al. (2012) examined the hydraulic data of this earthquake at the Choshi offshore area in detail. Figure 2 shows the variation of the wave height at an observation point. A massive tsunami struck at that observation point only 4 min after the largest aftershock occurred. The tsunami attack and the largest aftershock occurred almost simultaneously. This study indicates that liquefaction caused by earthquakes may occur when tsunami strikes. Actually, it was confirmed that the ground liquefied when the tsunami struck, as shown in Fig. 3.

Fig.2.

Fig.3.

Furthermore, Nagasaka et al. (2012) and Tonkin et al. (2003) pointed out that liquefaction might enhance the scour. Based on these reports, there is a possibility that the ground behind coastal dikes is eroded by tsunami easily when liquefaction occurs.

Although the above studies on the scour caused by tsunami and liquefaction caused by earthquakes have been conducted separately, the combined effects of liquefaction and scouring are poorly known. Moreover, large-scale earthquakes with a magnitude of around eight (such as the Tokai, Tonankai and Nankai earthquakes) are expected to occur with a high probability within 30 years (The Headquarters For Earthquake Research Promotion, 2016). Therefore, countermeasures against tsunami disaster caused by such large-scale earthquakes are important, and it is necessary to clarify the influence of liquefaction on the scour behind the coastal dikes. In the present study, flume experiments are conducted to clarify the influence of liquefaction on the scour. In particular, we focus on the variation of the scour profile (maximum scour depth, scour length and scour area) due to liquefaction.

Experimental Setup

Experimental apparatus

Schematic diagrams of the experimental apparatus are shown in Fig. 4; the scale of the experimental apparatus was 1/50. The experimental apparatus comprised a flume, coastal dike model, sand bed and water tank. The flume was 2.0 m long and 0.3 m wide and made of acrylic to observe the scour process. The coastal dike model was 0.2 m long, 0.1 m high and 0.3 m wide (5 m high in the real scale). The cross-section of the coastal dike model, corresponding to half of the slope, was determined based on coastal dikes in the Miyagi prefecture, which had been repaired after the earthquake. The sand bed was 0.5 m long, 0.2 m high and 0.3 m wide, and three pore-water pressure gauges were placed on the acrylic wall.

In the experiments, liquefaction was controlled by upward seepage, which was induced by the head difference between the water tank and the sand bed. The hydraulic gradient of the sand bed was $i = H/L$. In Fig. 4 (b), H is the difference in the total head, and L is

the height of the sand bed. The hydraulic gradient of the sand bed depended on the elevation of the water tank.

Fig.4.

Experimental conditions

Silica sand was used in the experiments. Its properties are shown in Table 1. The sand bed was made by water pluviation method in order to achieve saturation of the sand, and the relative density of the sand bed was about 30%. Table 2 shows the experimental conditions. Six types of the hydraulic gradients and two flow rates of q = 0.5 and 1.0 (L/s) were applied. The scour process and the scour profile were recorded by a video camera for 1 min. The duration of the overflow was about 7 min in the real scale. The maximum scour depth and the scour length were determined from the image captured by the video camera, as shown in Fig. 5.

Table 1

Table 2

Fig.5.

Upward Seepage and Excess Pore-water Pressure

Figure 6 shows the relationship between the hydraulic gradient and the flow rate of the upward seepage. It was observed that the flow rate of the upward seepage increased linearly with the hydraulic gradient. Figure 7 shows the relationship between the excess pore-water pressure in the sand bed and the depth from the bed surface. The effective overburden pressure was calculated from the submerged unit weight of the silica sand. The excess pore-water pressure increased with the hydraulic gradient and was approximately equal to the effective overburden pressure at i = 1.0. Thus, the effective

stress on the sand bed and liquefaction could be controlled by the hydraulic gradient. Moreover, although the critical hydraulic gradient calculated from the Terzaghi equation was 0.86, the critical hydraulic gradient in the present experiments was 1.0, due to the influence of the acrylic wall and the head loss between the sand bed and the water tank.

Fig.6.

Fig.7.

Results and Discussion

Influence of Liquefaction on Scour during the Initial Stage (1~10 s)

The scour profiles during the initial stage of the experiments are described for Series 2 (q = 1.0 L/s). Figure 8 shows the scour profiles at 1 s for i = 0.0 and i = 1.0. The scour profiles are completely different between i = 0.0 and i = 1.0. The formed scour hole for i = 0.0 has a semi-circular shape. Conversely, the scour hole for i = 1.0 is elongated and inclined obliquely. The overflow water sticks into the slope at the downstream part of the scour hole. This can be attributed to the increase in the fluidity of the sand bed due to liquefaction. These trends can be observed only for i = 1.0.

Fig.8.

Figure 9 shows the scour profiles at 8 s for i = 0.0 and i = 1.0. In addition, the scour profiles at 9 s and 10 s are also shown in Fig. 9 with dashed lines. For i = 0.0, the scour hole expands downstream and maintains a semi-circular shape. Conversely, the surface shape of the sand bed, for i = 1.0, changes continually by the increase in the fluidity of the sand bed. The surface of the sand bed becomes undulating. Furthermore, the slope at the downstream part of the scour hole is almost vertical. These trends are observed for i = 0.6, 0.8 and 1.0. Therefore, liquefaction has a significant impact on the scour profile during the initial stage of scouring.

Fig.9.

Scour Profile at each Hydraulic Gradient

Figure 10 shows the time variation of the scour length and the maximum scour depth at each hydraulic gradient. It can be observed that the scour length and the maximum scour depth change drastically from 0 to 10 s. After 10 s, the variation of the scour length and the maximum scour depth becomes small. The results show that the rate of increase in the scour length and the maximum scour depth decreases with time. In both cases, the scour length for i = 0.6, 0.8 and 1.0 becomes longer than that for i = 0.0, at any time. The results show that the scour hole expands downstream at high hydraulic gradients. This trend can be attributed to slope failures due to the reduction of the effective stress of the sand bed. Slope stability is determined by the balance between shear stress and shear strength. Shear strength decreases with the reduction of the effective stress, and the sediment under low-effective stress conditions behaves like a fluid. Consequently, slope failures and the expansion of the scour hole occur at high hydraulic gradients. Especially, when the hydraulic gradient is equal to 1.0, the scour-length increasing rate is obviously high. The scour length for i = 1.0 at the end of the experiment is 1.20 times longer in q = 0.5 and 1.59 times longer in q = 1.0, compared to i = 0.0. In both cases, the maximum scour depth for i = 0.6, 0.8 and 1.0 becomes smaller than that for i = 0.0, at any time. This trend can be attributed to backfilling of the scour hole. First, slope failures occur at high hydraulic gradient through the above-mentioned mechanism. Then, the scour hole is backfilled with sand from the slope failures. As a result, the maximum scour depth decreases. The maximum scour depth for i = 1.0 at the end of the experiment is 0.75 times smaller in q = 0.5, and 0.77 times smaller in q = 1.0, compared to i = 0.0.

Fig.10.

Influence of Liquefaction on Scour Area

In order to evaluate the influence of liquefaction quantitatively, we calculate the scour area at each hydraulic gradient. In past studies, the scour area under the original bed line was used as one of the evaluation methods (Mitobe et al., 2014). However, scouring far from a coastal dike does not affect the stability of the dike, whereas scouring near a coastal dike has a serious impact on the stability. In other words, even if the scour areas are equal to each other, the stability varies depending on the location of the scour. Therefore, it is necessary to consider the range, at which the stability is affected. In this study, the stable of the scour area was determined based on the "2*H* rule" (Minister of Land, Infrastructure, Transport and Tourism, 2011). When underground structures (e.g. buried pipeline and manhole) are placed near the foot of the dike, the following points must be considered according to the 2*H* rule: 1）Underground structures should be at least 20 m away from foot of the dike. When the height of the underground structures is less than 10 m, the structures should be 10 m away from the foot of the dike. 2）In other cases, underground structures should be placed outside the 1:2 line. The concept of the 2*H* rule is shown in Fig. 11. Underground structures should not be placed in the shaded area, because the stability of the coastal dikes and water leaks are affected there. Based on 2*H* rule, the scour inside the shaded area is determined as the scour area in this study.

Fig.11.

Figure 12 shows the relationship between the hydraulic gradient and the scour area at 10 s, 30 s and 1 min. In all cases, the scour area for i = 0.6, 0.8 and i = 1.0 becomes smaller than that for i = 0.0, at any time. The scour profile at a high hydraulic gradient

is shallow and wide due to slope failures caused by the reduction of the effective stress. As a result, the scour area near the foot of the dike becomes small. The scour area for i = 1.0 at the end of the experiment is 0.55 times smaller in q =0.5, and 0.64 times smaller in q = 1.0, compared to the values for i = 0.0. In previous studies, it has been reported that the scour is enhanced by liquefaction. However, this trend is not seen in this study. On the contrary, when the hydraulic gradient, that is, the degree of liquefaction is high, the scour area becomes small.

Fig.12.

Conclusions

In order to clarify the influence of liquefaction on the scour behind coastal dikes due to tsunami overflow, flume experiments were conducted. The following conclusions were obtained.

1. The scour profile for i = 0.0 at 1 s has a semi-circular shape. In contrast, the scour profile for i = 1.0 at 1 s is elongated and inclined obliquely. The overflow water sticks into the slope at the downstream part of the scour hole.
2. The scour hole for i = 0.0 expands maintaining a semi-circular shape. Conversely, the surface shape of the sand bed changes continually for i = 1.0. The undulating surface of the sand bed and the vertical slope downstream of the scour hole are observed. Therefore, liquefaction has a significant impact on the scour profile during the initial stage of scouring.
3. In q = 0.5 and 1.0 L/s, the scour length for i = 0.6, 0.8 and 1.0 becomes longer than that for i = 0.0, at any time. The scour length for i = 1.0 at the end of the experiment is 1.20 times longer in q = 0.5 and 1.59 times longer in q = 1.0 compared to i = 0.0.
4. In q = 0.5 and 1.0 L/s, the maximum scour depth for i = 0.6, 0.8 and 1.0 becomes smaller than that for i = 0.0 at any time. The maximum scour depth for i = 1.0 at the

end of the experiment is 0.75 times smaller in q = 0.5 and 0.77 times smaller in q = 1.0 compared to i = 0.0.

5. Based on 2H rule, the scour area, which affects the stability of coastal dikes, was calculated. In q = 0.5 and 1.0 L/s, the scour area for i = 0.6, 0.8 and 1.0 becomes smaller than that for i = 0.0, at any time. The scour area for i = 1.0 at the end of the experiment is 0.55 times smaller in q = 0.5 and 0.64 times smaller in q = 1.0 compared to i = 0.0.

References

Fukumoto, Y., Sukegawa, H., Iwamae, N. and Ikeya, T. (2012). "The 2011 off the Pacific coast of Tohoku Earthquake tsunami hydraulic data observed at Choshi offshore." *Journal of Japan Society of Civil Engineers*, 69(2), 1-5 (in Japanese).

Hatogai, S., Suwa, Y. and Kato, F. (2008). "Hydraulic model experiments on scour landward of the coastal dike induced by tsunami overflow." *Journal of Japan Society of Civil Engineers*, 68(2), I_406-I_410 (in Japanese).

Iiboshi, T., Maeno, S., Yosida, K. and Takata, D. (2014). "Effect of Shape of Landward Slope Protection and Toe Protection Works of Coastal Dikes on Landward Bed Scouring due to Tsunami Overflow." *Journal of Japan Society of Civil Engineers*, 70(2), I_966-I_970 (in Japanese).

Iiboshi, T., Maeno, S., Yosida, K., Takata, D. and Yamaura, A. (2015). "Effects of landward slope protection and toe protection work shape at coastal dikes on landward

bed scouring caused by tsunami overflow." *E-proceedings of the 36th IAHR World Congress*, Hague, Netherlands, IAHR.

Kato, F., Suwa, Y., Watanabe, K. and Hatogai, S. (2012). "Mechanisms of coastal dike failure induced by the Great East Japan earthquake tsunami." *Proceeding of 33rd International Conference on Coastal Engineering*, Santander, Spain, ICCE.

Kawasaki, K. (2012). "Fundamental characteristics of tsunami and tsunami Disaster due to the 2011 off the Pacific coast of Tohoku Earthquake." *The Japanese Society for Multiphase Flow*, 26(1), 11-18 (in Japanese).

Mikami, T., Shibayama, T. and Esteban, M. (2012). "Field survey of the 2011 Tohoku Earthquake and tsunami in Miyagi and Fukushima prefectures." *Coastal Engineering Journal*, 54(1), 1-26.

Minister of Land, Infrastructure, Transport and Tourism (2011). "Guideline of technical investigation for permitted structure." http://www.mlit.go.jp/river/shishin_guideline/kasen/pdf/kyokakousakubutu_tebiki.pdf, (accessed 2016/10/03) (in Japanese).

Mitobe, Y., Adityawan, MB., Tanaka, H., Kawahara, T., Kurosawa, T. and Otsushi, K. (2014). "Experiments on scouring behind coastal dikes induced by tsunami overflow." *Journal of Japan Society of Civil Engineers*, 70(4), I_1147-I_1152 (in Japanese).

Nagasaka, Y., Harry, Y., Nakao, H., Sato, S., Tajima, Y. and Yamanaka, Y. (2012). "Study on the erosion mechanisms of soil embankment by tsunamis." *Journal of Japan Society of Civil Engineers*, 68(2), I_1331-I_1335 (in Japanese).

Tanimoto, R. and Tokida, K. (2012). "Study on structure of dug pool eroded by tsunami flood and its tsunami-reduction function." *International Symposium on Earthquake Engineering*, 1, 143-150.

The Headquarters for Earthquake Research Promotion (2016). "List of long-term evaluation." http://www.jishin.go.jp/evaluation/long_term_evaluation/lte_summary/, (accessed 2016/10/03) (in Japanese).

Tokida, K. and Koizumi, K. (2011). "Lessons from tsunami damage and discussion on hard countermeasures Part1." *Geotechnical Engineering Magazine*, 59(8), 36-42 (in Japanese).

Tokida, K. and Tanimoto, R. (2014). "Lessons for countermeasures using earth structures against tsunami obtained in the 2011 off the Pacific coast of Tohoku Earthquake." *Soils and Foundations*, 54(4), 523-543.

Tonkin, S., Yeh, H., Kato, F. and Sato, S. (2003). "Tsunami scour around a cylinder." *Journal of Fluid Mechanics*, 496, 165-192.

Figure 1. Scour hole behind a coastal dike (modified from Iiboshi et al., 2014).

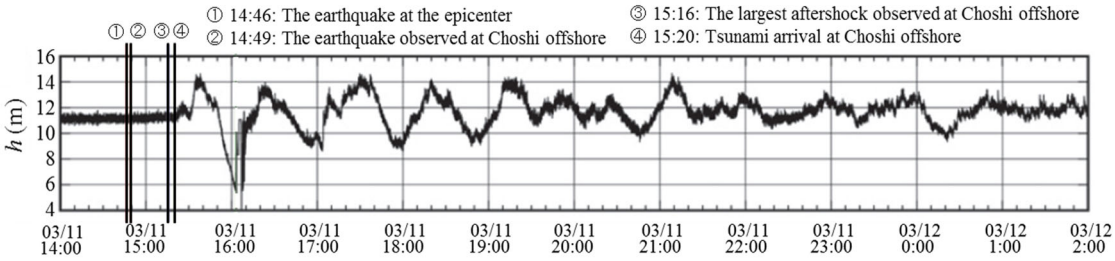

Figure 2. Variation of wave height at Choshi offshore area (modified from Fukumoto et al., 2012).

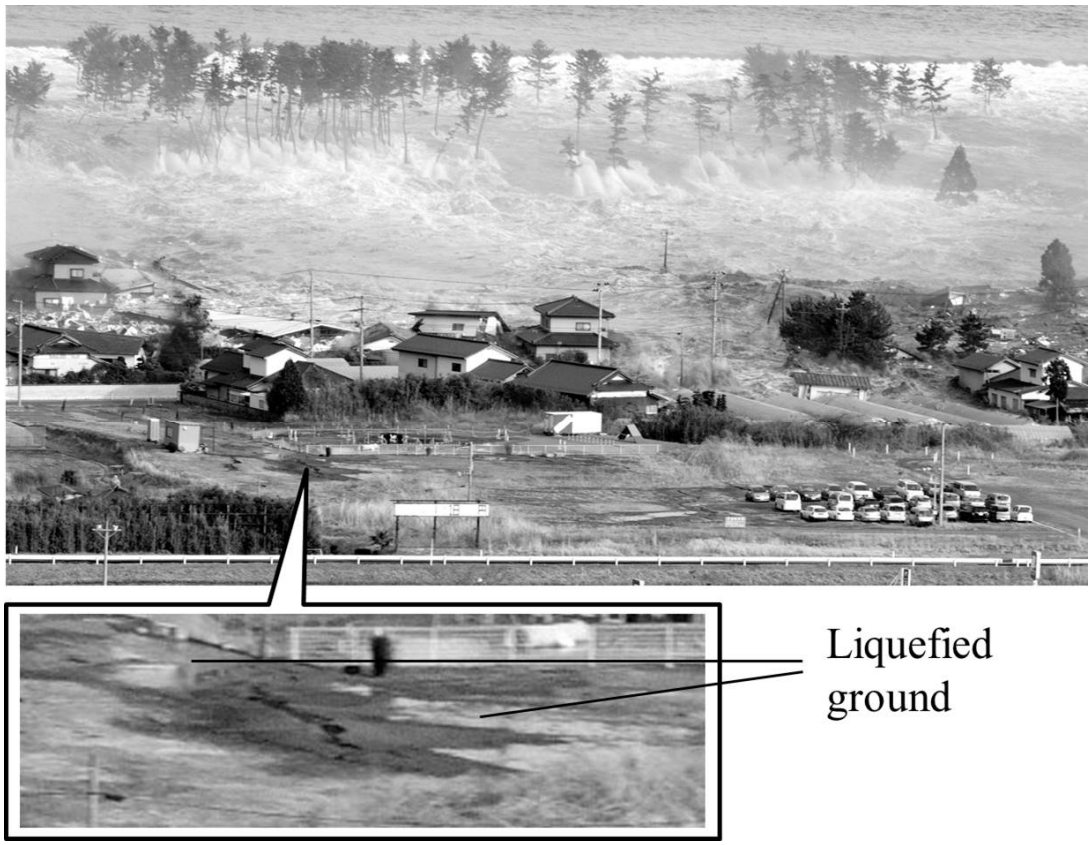

Figure 3. Ground liquefies before a tsunami strikes (Natori City, Miyagi Prefecture).

Photo courtesy of Kyodo News Service.

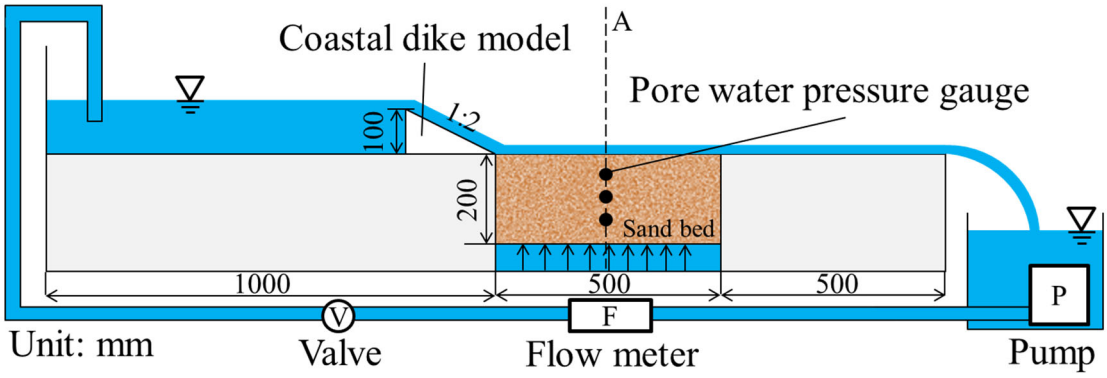

(a) Side view of the experimental apparatus without a water tank.

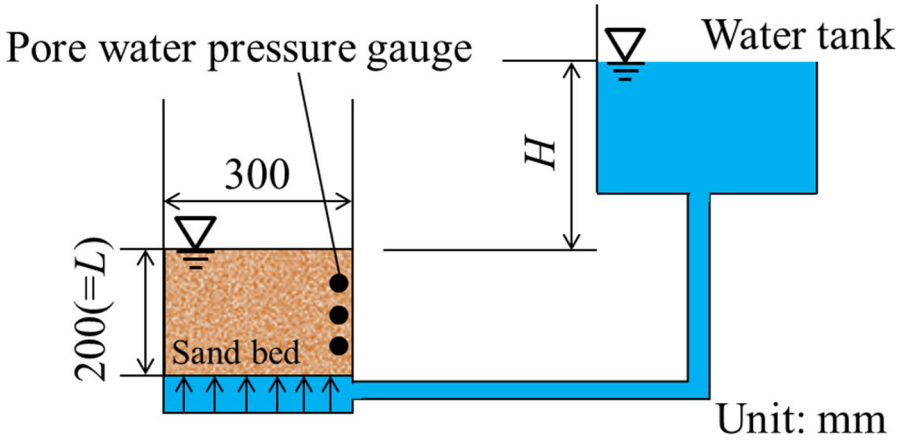

(b) Cross section of A.

Figure 4. Experimental apparatus.

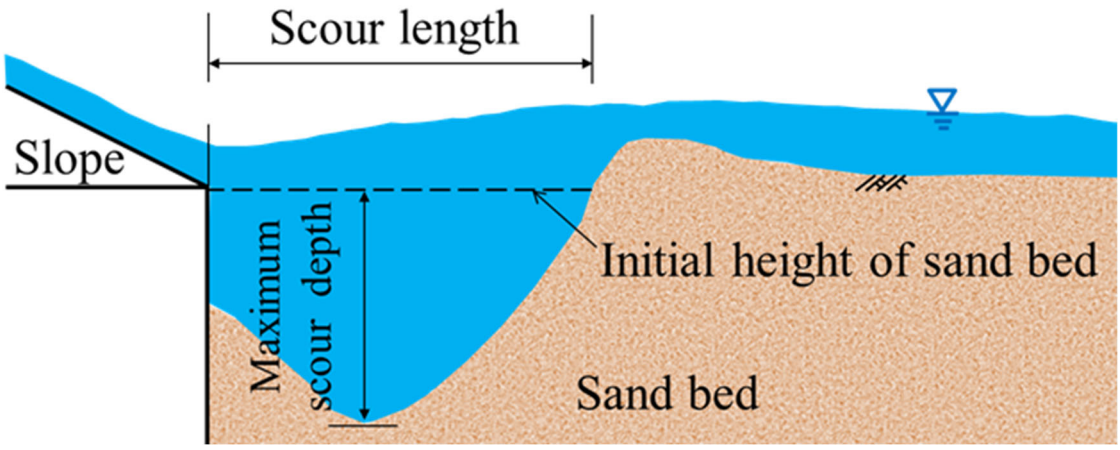

Figure 5. Definition of maximum scour depth and scour length.

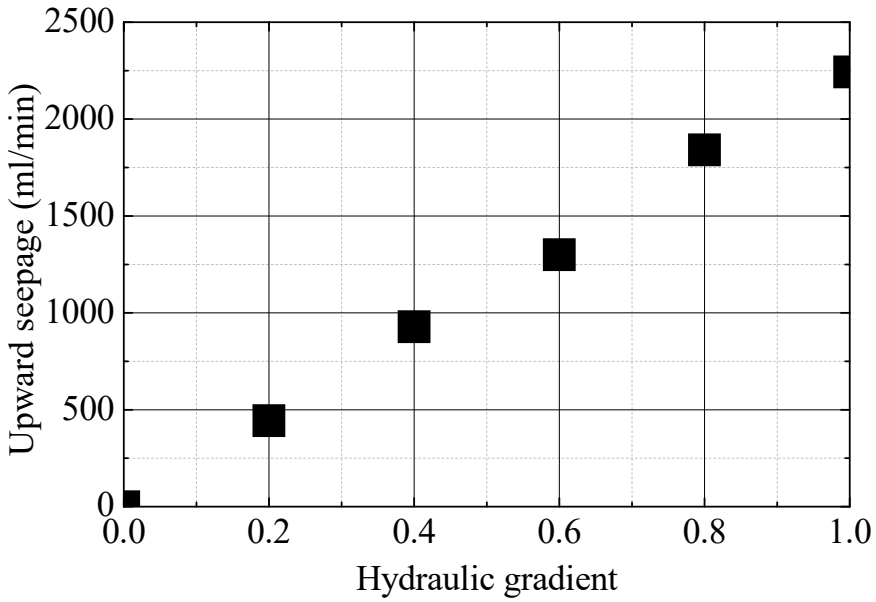

Figure 6. Relationship between hydraulic gradient and upward seepage.

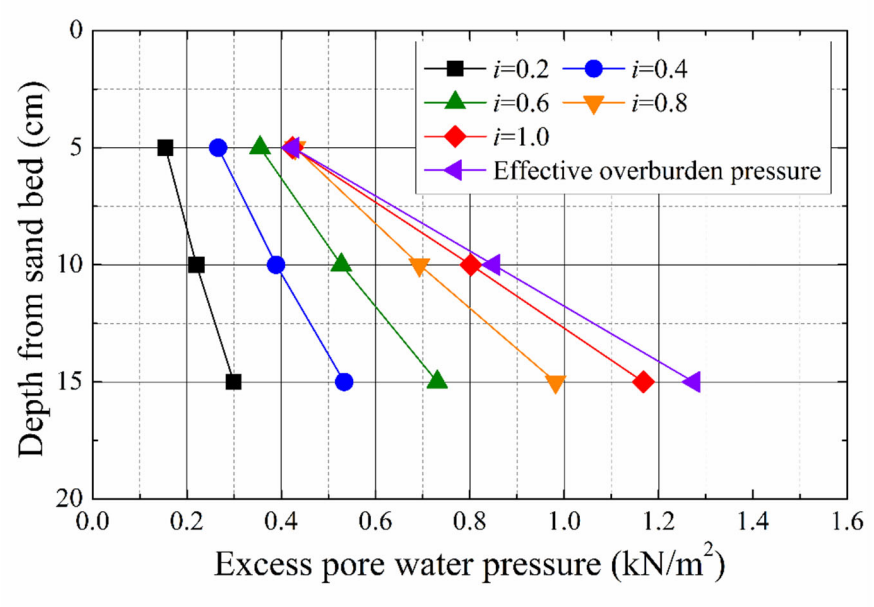

Figure 7. Relationship between excess pore-water pressure and depth from sand bed.

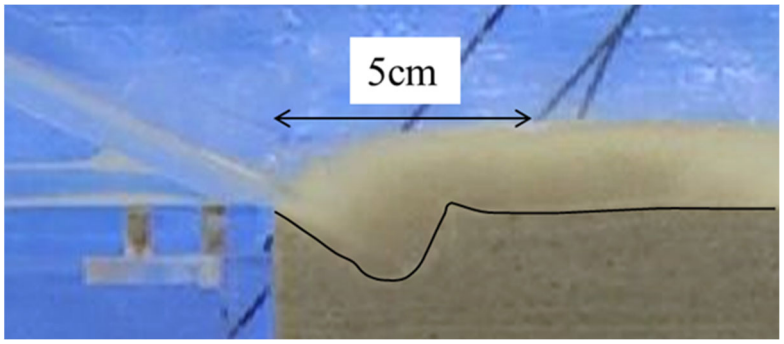

(a) i = 0.0

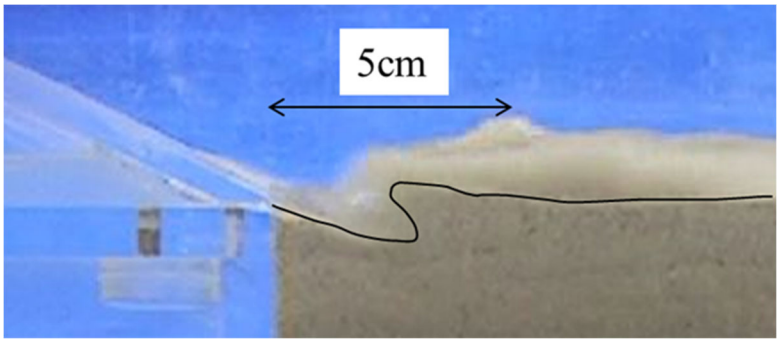

(b) i = 1.0

Figure 8. Scour profiles at 1 s for i = 0.0 and i = 1.0.

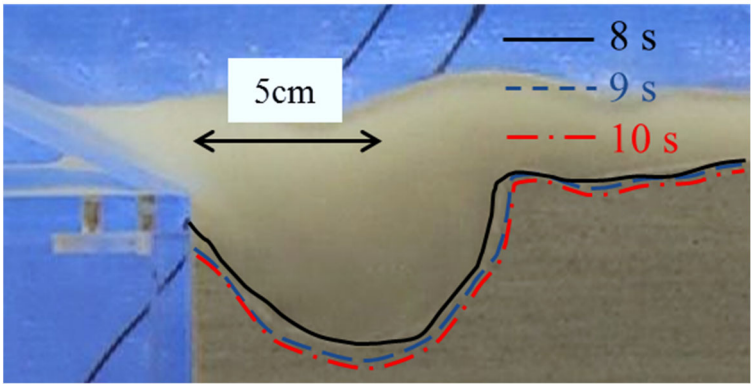

(a) i = 0.0

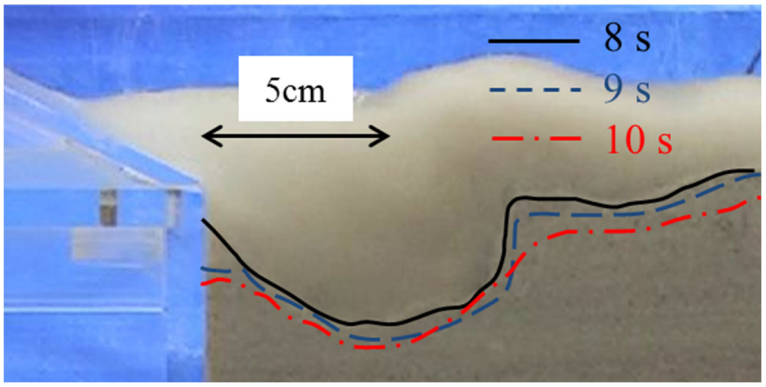

(b) i = 1.0

Figure 9. Scour profiles at 8, 9 and 10 s for i = 0.0 and i = 1.0.

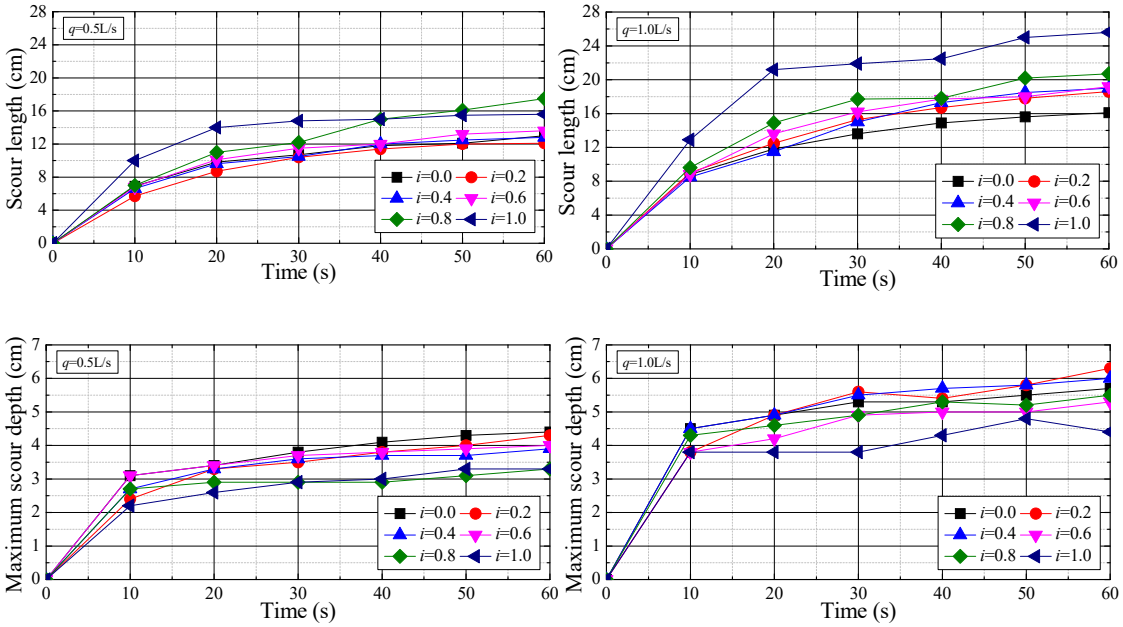

(a) q = 0.5 L/s (b) q = 1.0 L/s

Figure 10. Time variation of scour length and maximum scour depth at each hydraulic gradient.

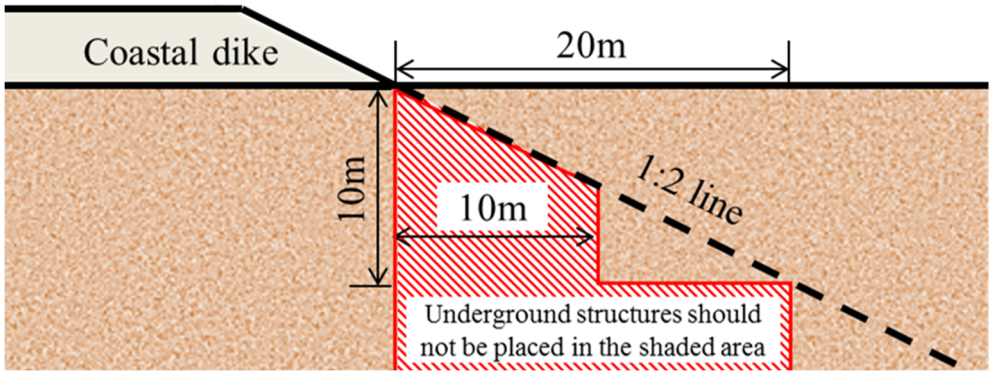

Figure 11. Concept of the 2*H* rule.

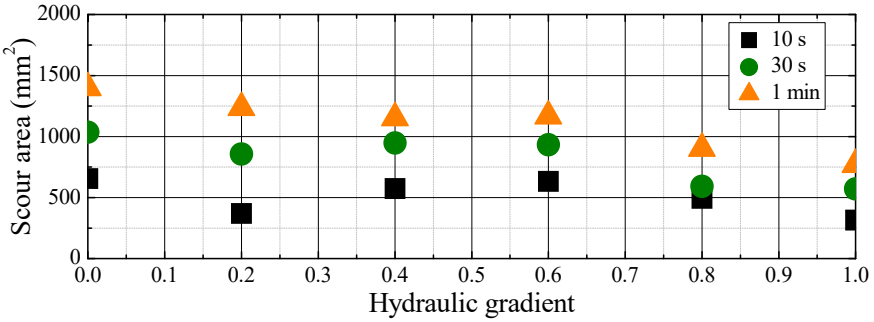

(a) q = 0.5 L/s

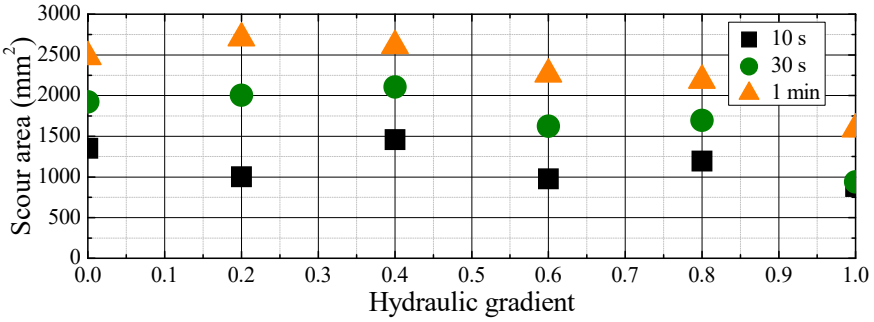

(b) q = 1.0 L/s

Figure 12. Relationship between hydraulic gradient and scour area.

Table 1. Properties of silica sand.

Density of soil particle ρ_s (g/cm^3)	2.63
Maximum dry density ρ_{max} (g/cm^3)	1.64
Minimum dry density ρ_{min} (g/cm^3)	1.30
50% grain size D_{50} (mm)	0.30
Uniformity index U_c	2.14

Table 2. Experimental conditions.

Series 1		Series 2	
Hydraulic gradient i	Flow rate q	Hydraulic gradient i	Flow rate q
0.0	0.5 (L/s)	0.0	1.0 (L/s)
0.2		0.2	
0.4		0.4	
0.6		0.6	
0.8		0.8	
1.0		1.0	

Funding

The work was supported by the JSPS under Grant in Aid for Young Scientists (B) number 15K18758.